Electronic Supplementary Material (ESI) for Physical Chemistry Chemical Physics.

Supplementary Information

First-principles calculations of bulk, surface and interfacial phases and properties of silicon graphite composites as anode materials for lithium ion batteries

Stéphane B. Olou'ou Guifo[a,b], Jonathan E. Mueller[a*], David Henriques[b], Torsten Markus[b]

[a]Volkswagen Group, Berliner Ring 2, D-38436, Wolfsburg, Germany

[b]Institute of Materials Science and Engineering, Mannheim University of Applied Sciences, Paul-Wittsack-Straße 10, D-68153, Mannheim, Germany

*corresponding author: jonathan.edward.mueller@volkswagen.de

A) Linearity between the formation energy and the mixing volume

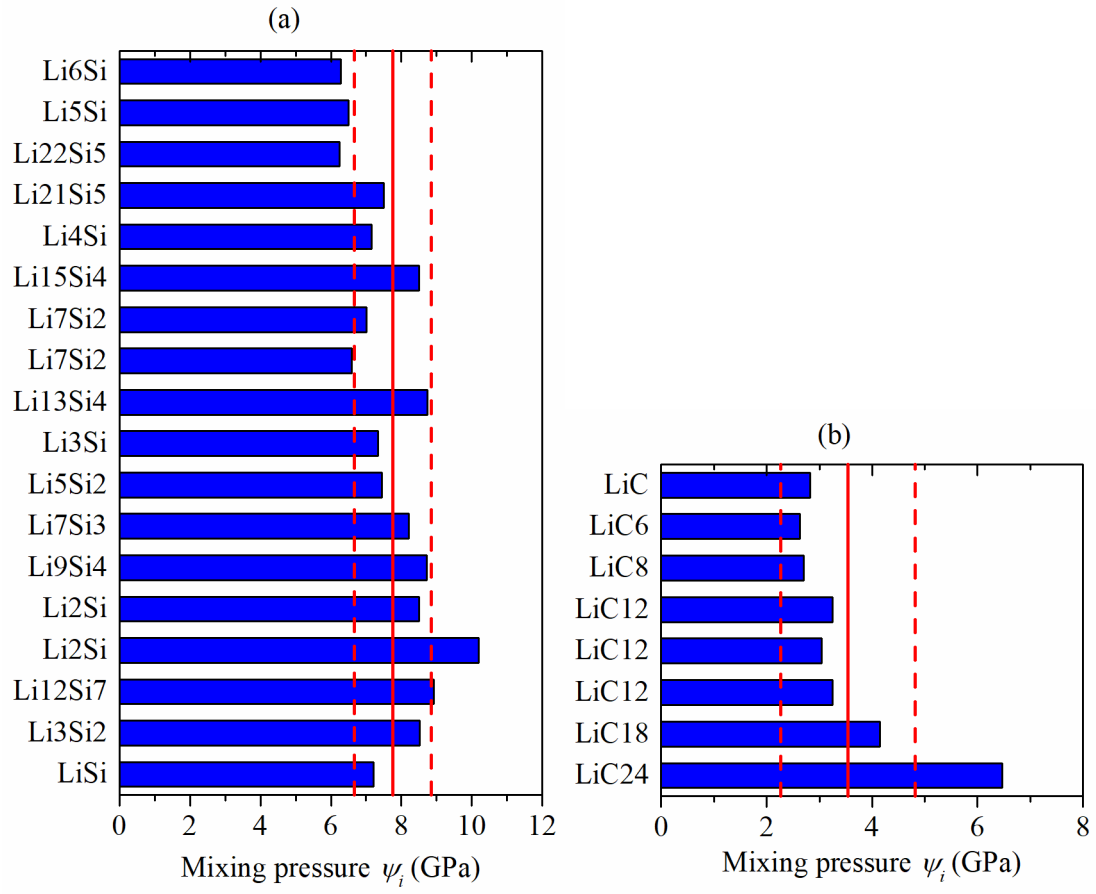

Fig. S.1: Mixing pressure defined as the ratio of the mixing energy and the mixing volume for stable and metastable (a) Li_XSi_{1-X} and (b) Li_YC_{1-Y} phases .

The red, solid lines represents the arithmetic value over all computed phases and the red, dashed lines are the standard deviations for the samples.

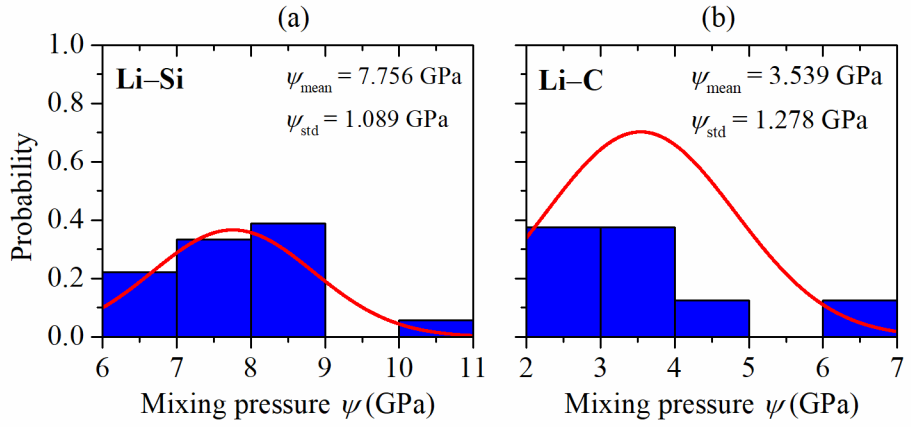

Fig. S.2: Probability distribution of the mixing pressure for the (a) Li–Si and (b) Li–C systems.

The red lines are the normal distribution functions based on the average values and standard deviations.

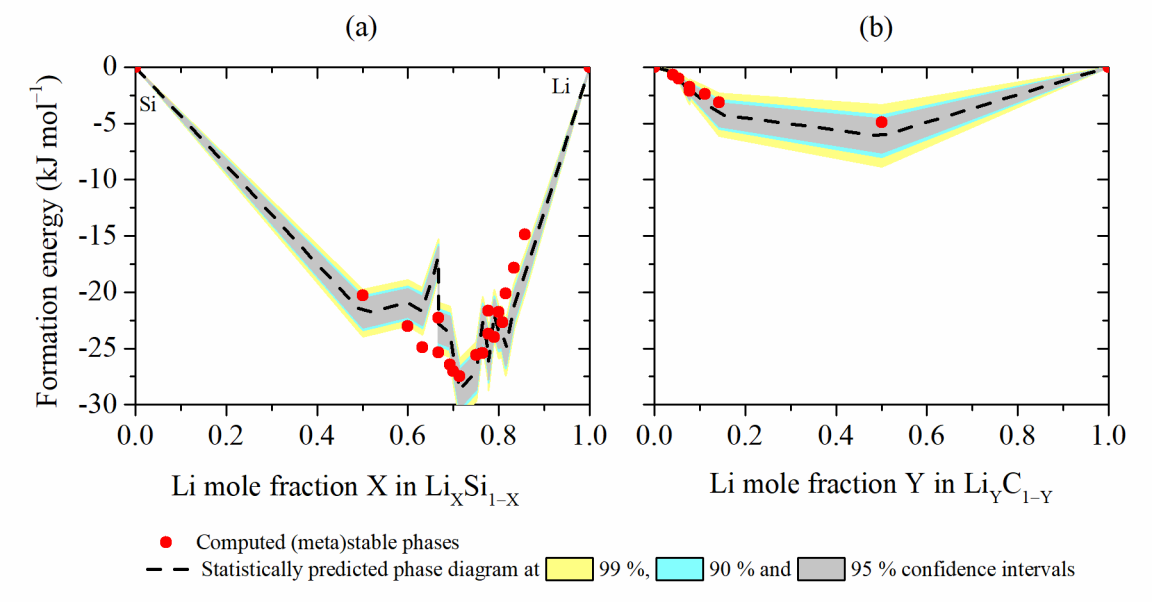

Fig. S.3: Ground state phase diagram spectrum for the Li–Si and Li–C systems from statistical predictions based on known binary phases.

A normal distribution, of the mixing pressure of the compounds around an excepted value of each of the binary systems is assumed. The mixing volume is used as input parameter for computing the mixing energy region at any predefined confidence interval.

B) Theoretical capacity of silicon and graphite anodes

Tab. S.1: Theoretical gravimetric and volumetric capacities of silicon and graphite from DFT results and from experiments.

The experimental (exp.) values are taken from the literature review of Liu *et al.*[1].

Anode system	Maximum volume expansion (%)	State of charge (SoC)	Gravimetric capacity (mA h g^{-1})	Volumetric capacity (mA h cm^{-3})
Silicon	291 ($Li_{21}Si_5$) 410 (exp. $Li_{22}Si_5$)	Delithiated (discharged)	4008 4200 (exp.)	9212 9660 (exp.)
		Lithiated (charged)	1967 2010 (exp.)	2458 2370 (exp.)
Graphite	12 12 (exp.)	Delithiated (discharged)	372 372 (exp.)	853 837 (exp.)
		Lithiated (charged)	339 339 (exp.)	760 747 (exp.)

C) Surface tensions of Li_xSi and Li_yC at various orientations and lithium contents

Tab. S.2: Surface tensions of graphite structures with respect to the initial periodic structure for various symmetries and lithium contents.

Phase	Surface orientation	Surface tension (J m^{-2})		
		DFT	optB86b	DFT-D2
C (hexagonal, $P6_3/mmc$)	(100) or (10$\bar{1}$0) (zigzag)	6.216	7.838	8.084
	(110) or (11$\bar{2}$0) (armchair)	3.920	5.095	5.241
	(0001)	–0.001	0.230	0.190
C (Cmme, orthorhombic)	(100) (armchair)	3.831	5.024	5.204
	(010) (zigzag)	7.190	8.968	9.355
	(001)	0.000	0.224	0.181
LiC_6 (hexagonal, P6/mmm)	(100) or (10$\bar{1}$0) (armchair)	3.492	3.797	3.955
	(110) or (11$\bar{2}$0) (zigzag)	3.338	4.547	4.677
	(0001) (C vs C)	–0.003	0.238	0.192
	(0001) (C vs Li)	0.340	0.565	0.707
	(0001) (Li vs Li)	0.643	0.783	0.871

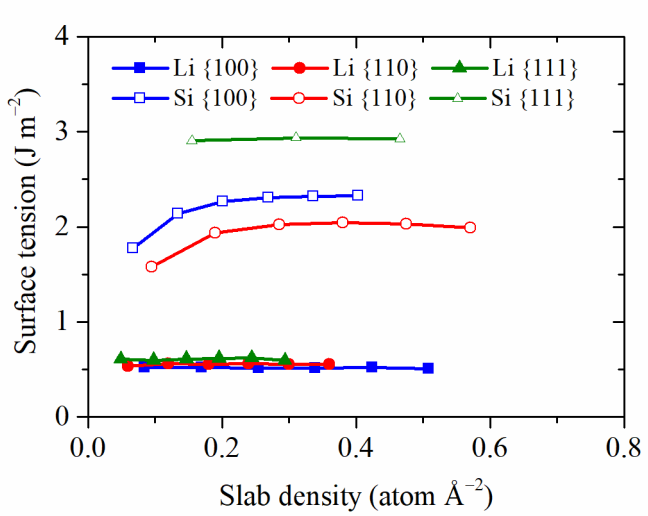

Fig. S.4: Surface tension as a function of the atomic loading density lithium and silicon slabs with different surface orientations.

The slabs with highest slab density are chosen as representative models for silicon and lithium in this work. They exhibit a convergence around 0.02 J m^{-2}. Each slab surface tension has a horizontal asymptote corresponding to the infinite loading density.

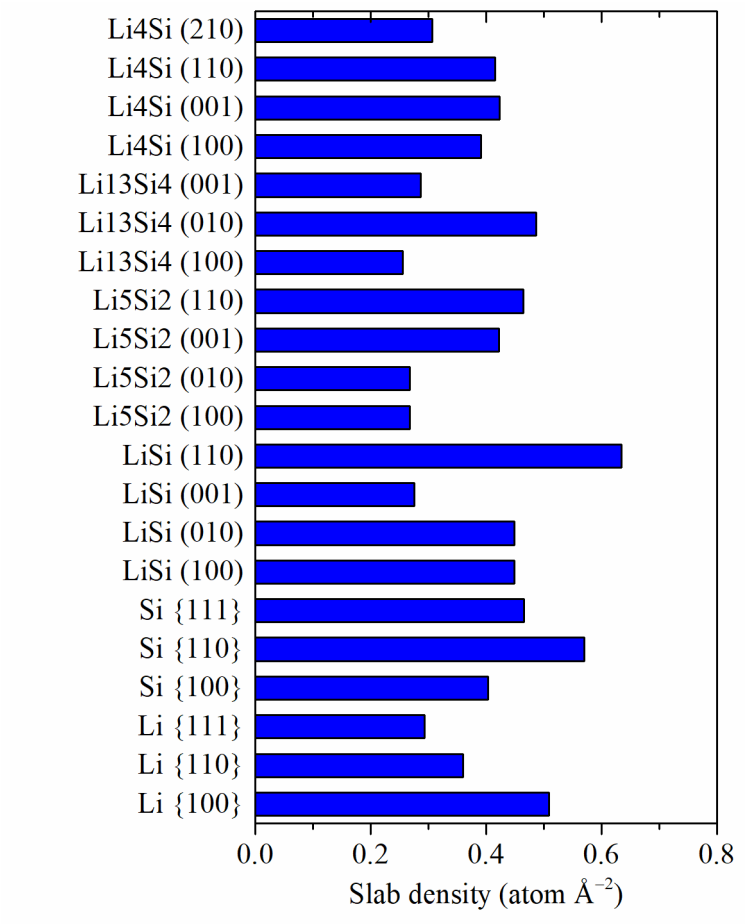

Fig. S.5: Slab density of simulated Li_xSi slabs.

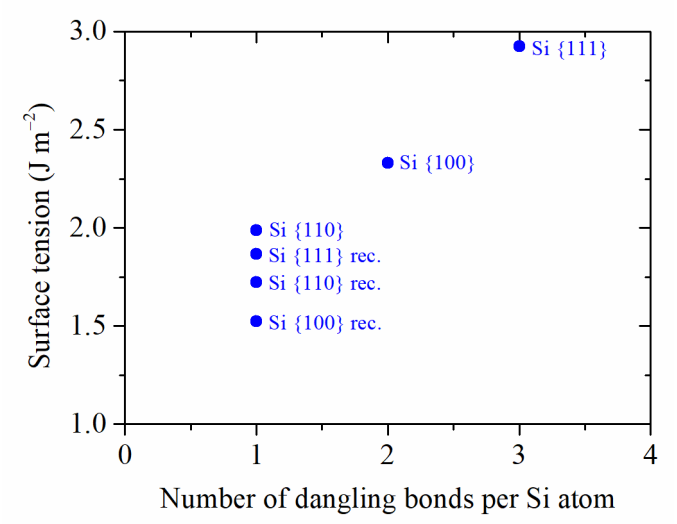

Fig. S.6: Thermally activated reduction of the dangling bonds of silicon surface atoms throughout AIMD simulations accompanied by the reduction of the surface tension.

Tab. S.3: Reconstruction of Li_xSi surfaces using AIMD for overcoming energy barriers and reach surface equilibrium.

AIMD simulations are carried out considering a NVE ensemble with an initial temperature of 500 K, a time step of 2 fs and a total time of 400 fs. GO stands for geometry optimization.

Phase	Surface	Surface tension from GO ($J\ m^{-2}$)	Surface tension from AIMD + GO ($J\ m^{-2}$)	Energy loss during surface reconstruction ($J\ m^{-2}$)
Si	{100}	2.329	1.525	0.804
	{110}	1.989	1.725	0.264
	{111}	2.925	1.815	1.110
LiSi	(100)	0.762	0.762	0.000
	(001)	1.117	1.117	0.000
	(110)	0.902	0.902	0.000
Li_5Si_2	(100)	1.093	0.982	0.111
	(001)	0.813	0.813	0.000
	(110)	0.964	0.964	0.000
$Li_{13}Si_4$	(100)	1.224	0.927	0.297
	(010)	0.963	0.963	0.000
	(001)	0.873	0.874	–0.001
Li_4Si	(100)	1.263	1.139	0.124
	(001)	0.918	0.965	–0.047
	(110)	0.686	0.686	0.000
	(210)	1.091	0.858	0.233

D) Charge density analysis in Li_xSi and Li_yC slabs

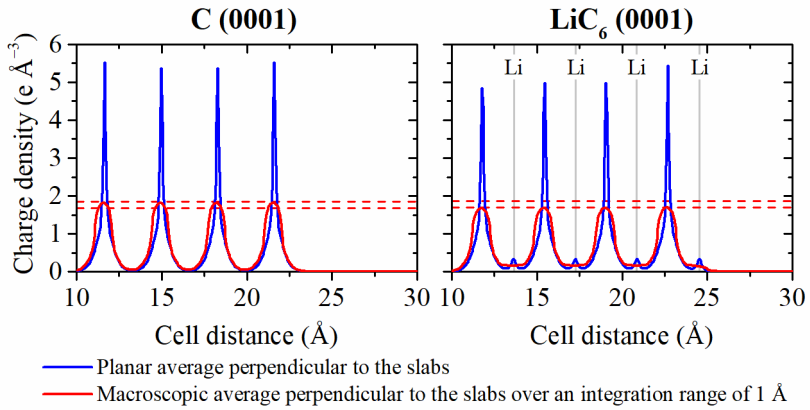

Fig. S.7: Total charge density of delithiated and lithiated graphite slabs as carbon and LiC_6, respectively with (0001) surface orientation.

The blue lines represent the total charge density averaged over planes parallel to the slab whereas the slightly smoothed red lines are the integrated total charge densities over a distance of 1 Å perpendicular to the slab. For LiC_6, a lithium termination is considered on the right slab side while the left side is without lithium in order to see the vacuum effects on both lithium adatoms and graphene layers.

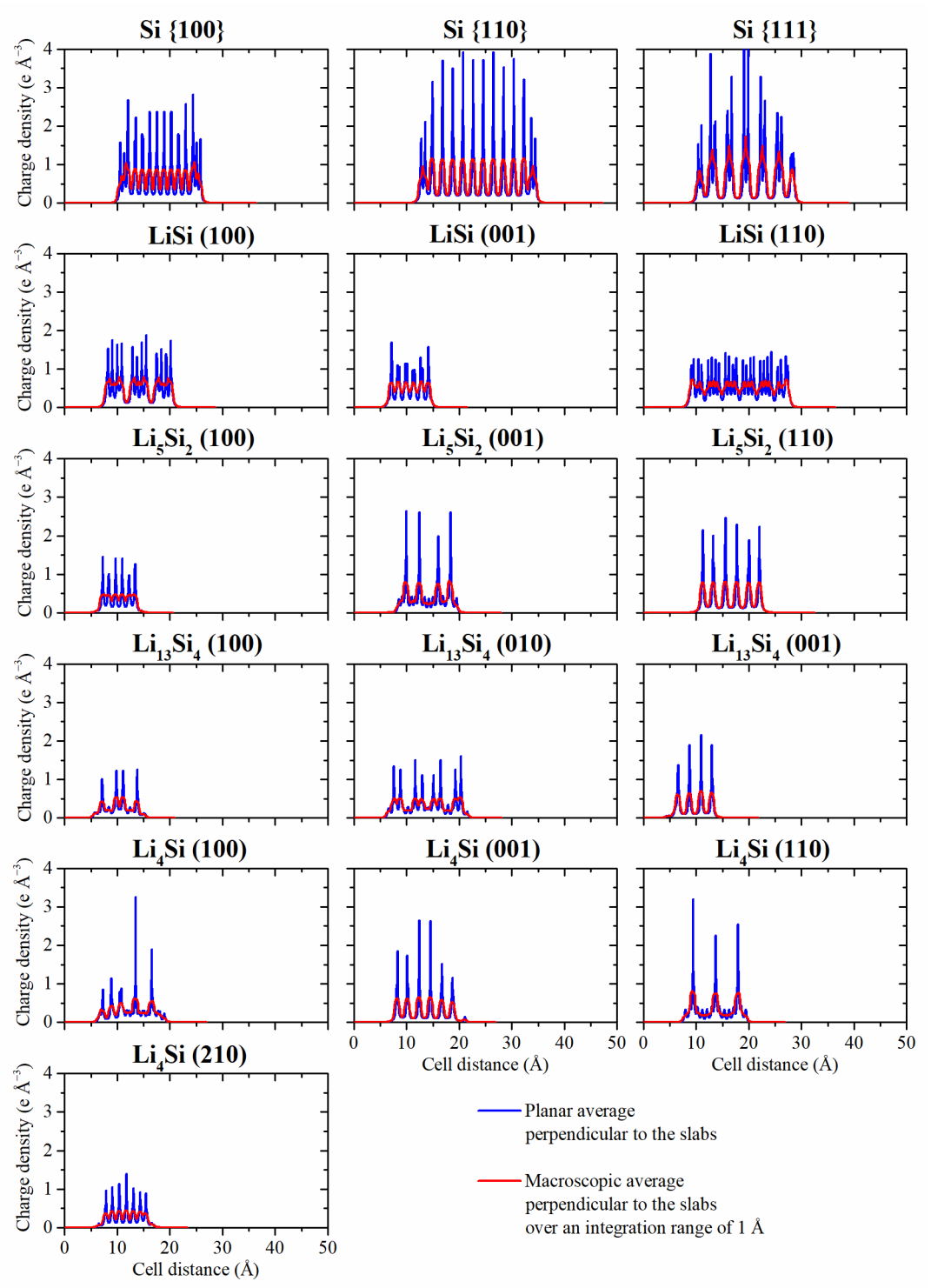

Fig. S.8: One-dimensional total charge density of Li_xSi slabs (x = 0; 1; 2.5; 3.25 and 4) with various surface orientations.

The blue lines represent the total charge density averaged over planes parallel to the slab whereas the slightly smoothed red lines are the integrated total charge densities over a distance of 1 Å perpendicular to the slab.

E) Effects of voids on the interface tension between Li_xSi and Li_yC phases

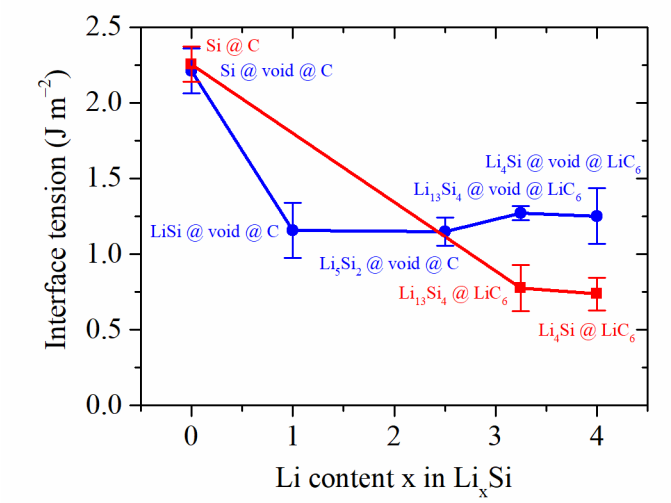

Fig. S.9: Averaged interface tensions of Li_xSi–Li_yC (red line with squares) and Li_xSi–void–Li_yC (blue line with circles) with various configurations as function for the lithium content in silicon.

Literature

(1) Liu, N.; Li, W.; Pasta, M.; Cui, Y. Nanomaterials for electrochemical energy storage. *Front. Phys.* **2014**, *9*, 323–350.